Fuelling efficiency and penetration of supersonic molecular beam injection in HL-2A tokamak plasmas

D.L. Yu*, C.Y. Chen, L.H. Yao, B.B. Feng, Y. Zhou, X.Y. Han, K.J. Zhao, J. Zhou, W.L. Zhong, Y. Huang, Yi Liu, L.W. Yan, Q.W. Yang, X.T. Ding, J.Q. Dong, X.R. Duan, Yong Liu
Southwestern Institute of Physics, Chengdu, China
*Email: yudl@swip.ac.cn

Abstract

The fuelling efficiency and penetration characteristics of supersonic molecular beam injection (SMBI) have been studied on HL-2A tokamak. The signals from the tangential D_α array and CCD camera clearly show that the SMBI from low field side (LFS) consists of a slow component (SC) and a fast component (FC). The FC can penetrate more deeply than the SC, such as 8.5 cm inside the last closed flux surface (LCFS), while the SC is around 4 cm. The penetration depth of the SC is weakly dependent on the line-averaged plasma density before injection and the backing pressure. Typical fuelling efficiency of LFS SMBI is 30~60% for the limiter configuration. It is more the variation of the decay time of the post-SMBI electron density than the different injection depth that is responsible for the large scatter of the measured fuelling efficiencies. The fuelling efficiency from high field side (HFS) is higher than that from LFS for the ohmic heating discharges; moreover, with ECRH power of 1.3MW, this trend becomes much more distinct indicating it is better for SMBI to fuel from HFS.

Keywords: Fuelling depth, Dα emission, fuelling efficiency, supersonic molecular beam injection

PACS Number: 28.52.Cx, 52.25.Ya

1. Introduction

Supersonic molecular beam injection (SMBI), as an effective fuelling method, was first successfully developed on HL-1M tokamak [1] and then widely adopted by other devices such as HL-2A, Tore Supra [2] and ASDEX-U [3] due to its high fuelling efficiency, simplicity of structure and low cost. It is reported that the fuelling efficiency ranges from 30~60% on Tore Supra [2]; and on ASDEX-U, fuelling efficiency is about 30% for L-mode and low density H-mode plasmas and is reduced to less than 15% in high density H-mode discharges[4].

On HL-2A, the SMBI can fuel plasma from both the low field side (LFS) with an electro-magnetic valve and the high field side (HFS) with a pneumatic valve, as shown in figure 1. The distance from plasma to HFS nozzle is several centimeters only, whereas the LFS is about 1.28 m. The relevant diagnostics around the SMBI are D_α arrays and CCD cameras. Two D_α arrays and a CCD camera are installed in the same cross-section with respect to the SMBI port. Besides, a 46-channel tangential D_α array monitors the half cross-section on the LFS with 0.9 cm spatial resolution and typical acquisition frequency of

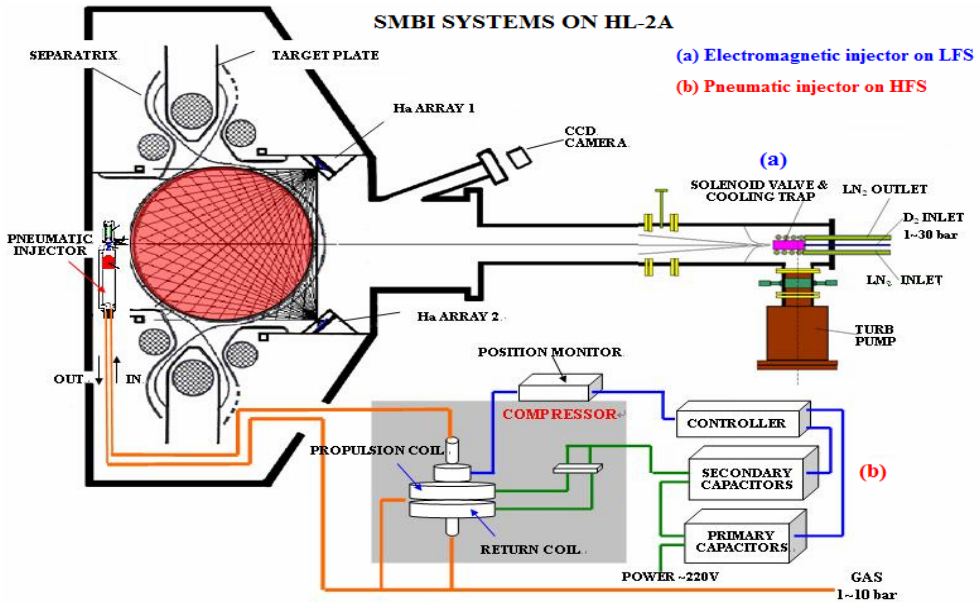

FIG. 1. Schematic arrangement of the SMBI and the relevant diagnostics.

200 kHz. In addition to the tangential array, a CCD camera can be utilized to study the penetration characteristics of LFS SMBI. The preliminary database of fuelling efficiency of LFS SMBI has been established [5]. Fuelling efficiency of LFS and HFS SMBIs are compared for shots with and without ECRH.

2. Fast and slow beam components

For each LFS pulse, there are two peaks on tangential D_α signal during an SMBI pulse. As shown in figure 2, the delay time with respect to the SMBI signal are 0.7 ms and 1 ms for the first peak and the second one, respectively, indicating that SMBI consists of two components, one is the fast component (FC) with velocity of 1.9 km/s and the other is slow component (SC) with velocity of 1.3 km/s only. The appearance of the FC is due to the utilization of the additional conical nozzle, which is installed on the valve to optimize the beam and make it more concentrated. The FC has not been observed before the installation of the conical nozzle, and by doping different percentage of hydrogen into deuterium the magnitude and velocity of the FC keeps almost no change; therefore, the reason inducing the FC can not be due to the isotope effect. In addition, the FC is also

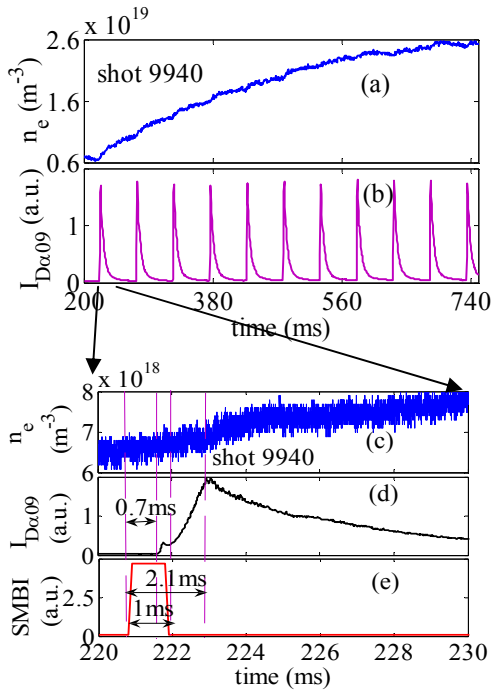

FIG. 2. Characteristics of the D_α emission monitored by the tangential array.
Time traces from top to bottom are: (a) line-averaged electron density; (b) D_α emission monitoring the molecular beam; their corresponding time extensions in (c) and (d); (e) SMBI controlling signal.

observed by H_α array on Heliotron J device.

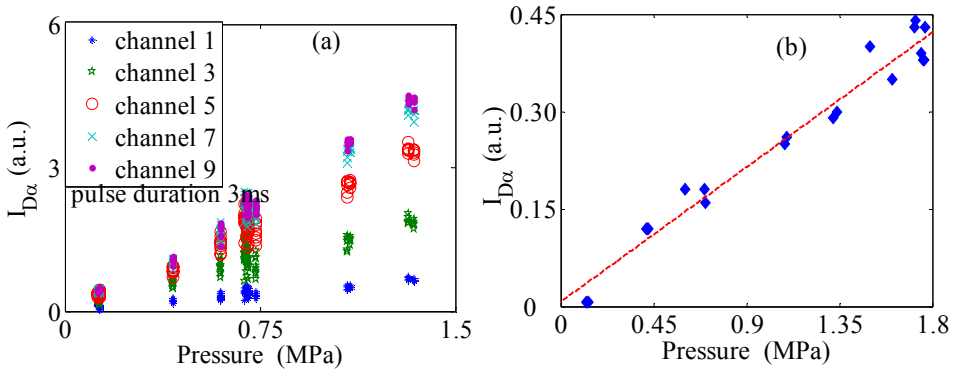

FIG. 3. Dependence of D_α emission intensity on injected deuterium inventory. (a) and (b) are the SC and FC, respectively.

3. D_α feature During SMBI

To study the feature of the FC, the D_α emission is analyzed. The dependence of D_α intensity on injected deuterium inventory is shown in figure 3. For the case of the SC, the time integrated D_α intensity is proportional to the backing pressure for each channel, as shown in figure 3(a). As the pulse duration is fixed at 3 ms, the injected inventory is proportional to the pressure. In other words, the time integrated D_α emission is proportional to the injected molecular inventory for the SC. As for the FC, the duration is about 0.3 ms only and the rising time is about the half; so that the time integrated D_α emission is replaced by the maximum intensity for the sake of simplicity. The maximum intensity of D_α is proportional to the backing pressure, as shown in figure 3(b). Since the duration of the FC is almost invariant, therefore, the D_α emission is proportional to the injected particles, which is the product of the backing pressure and the pulse duration. Estimated from the intensity of D_α, the SC is the major part of the SMBI, whereas the FC is the minority. And hence the fuelling ability of the FC is very limited.

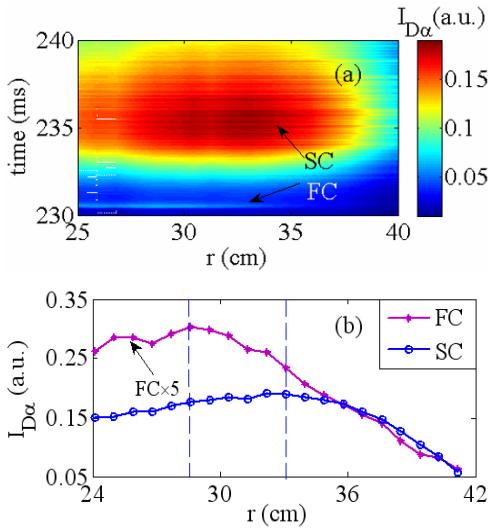

FIG. 4. Typical penetration features of the FC and SC for the LFS SMBI. (a) *Contour plot and* (b) *maximum D_α along radius of the SC and FC, respectively.*

4. Penetration characteristics of the FC and SC

The penetration characteristics of the SC and FC are quite different, as shown in figure 4. The maximum D_α intensity of the FC locates more deeply than the SC, such as 8.5 cm inside the last closed flux surface (LCFS), while the SC penetrates around 4 cm.

To study the influence of plasma density on SMBI penetration, a series of 11 pulses is injected and the plasma density increases from 0.6 to 2.6 $\times 10^{19}$ m^{-3}, as shown in figure 2. The maximum D_α profiles versus minor radius are shown in figure 5. With the increase of plasma density, the maximum D_α intensity of two channels outside minor radius of 34 cm becomes flat, indicating there exists a slight influence from background plasma density on the penetration of SC, but not very heavily.

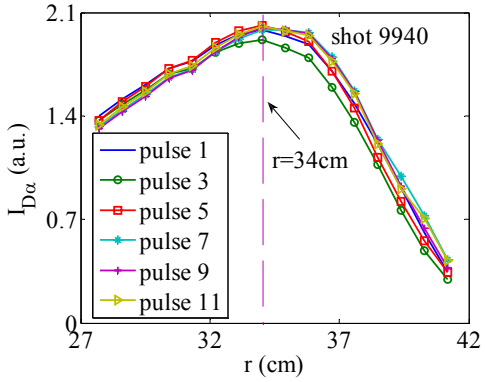

FIG. 5. Maximum D_α intensity versus minor radius in shot 9940.
The SMBI parameters are pulse duration of 1 ms, backing pressure of 1.7 MPa and the time interval of 50 ms between pulses.

Another interesting phenomenon is that the injection depth is weakly dependent on the backing pressure of the SMBI, as shown in figure 6. Figures 6(a) and (b) show the maximum D_α intensity locates around channels 14 and 9 for the FC and SC, corresponding to the minor radii of 29.5 cm and 34 cm, respectively. Although the backing pressure of the seven shots increases from 0.126 MPa to 1.7 MPa, the maximum intensity of D_α locates at the same channel for the SC and varies only about one or two channels for the FC (the spatial resolution of tangential D_α array is 0.9 cm).

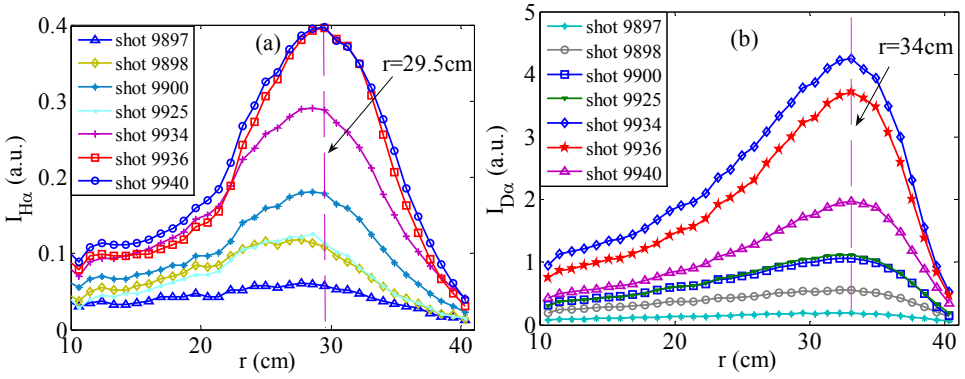

Figure 6. Dependence of the penetration depth on backing pressure for the FC and SC. The maximum D_α intensity is induced by the FC in (a) and by the SC in (b).
Backing pressures for shots 9897, 9898, 9900, 9925, 9934, 9936, 9940 are 0.126, 0.416, 0.6, 0.422, 1.32, 1.5 and 1.7 MPa. The pulse durations are 5 ms, 2 ms and 1 ms for shot 9925, 9936 and 9940, the other are 3 ms, respectively.

As a complement of the tangential D_α array, a CCD camera is alternatively utilized to observe the interaction between SMBI and the plasma with typical exposure time of 0.3 ms. Because of the frame-transfer rate limitation of the CCD camera, the pictures are captured shot by shot by changing the delay time with respect to the SMBI trigger signal. Figure 7 shows a typical evolution of the SMBI from LFS. Figures 7(a)~(h) correspond to different time phases depicted in figure 7(i), and each is taken in individual shot. Figure 7(i) is the D_α measured by a single-channel detector. The backing pressure of the SMBI keeps invariant, such as 0.75

MPa, and the electron density in figures 7(b)~(h) varies in the range of 1.6~2.2 $\times 10^{19}$ m^{-3}.

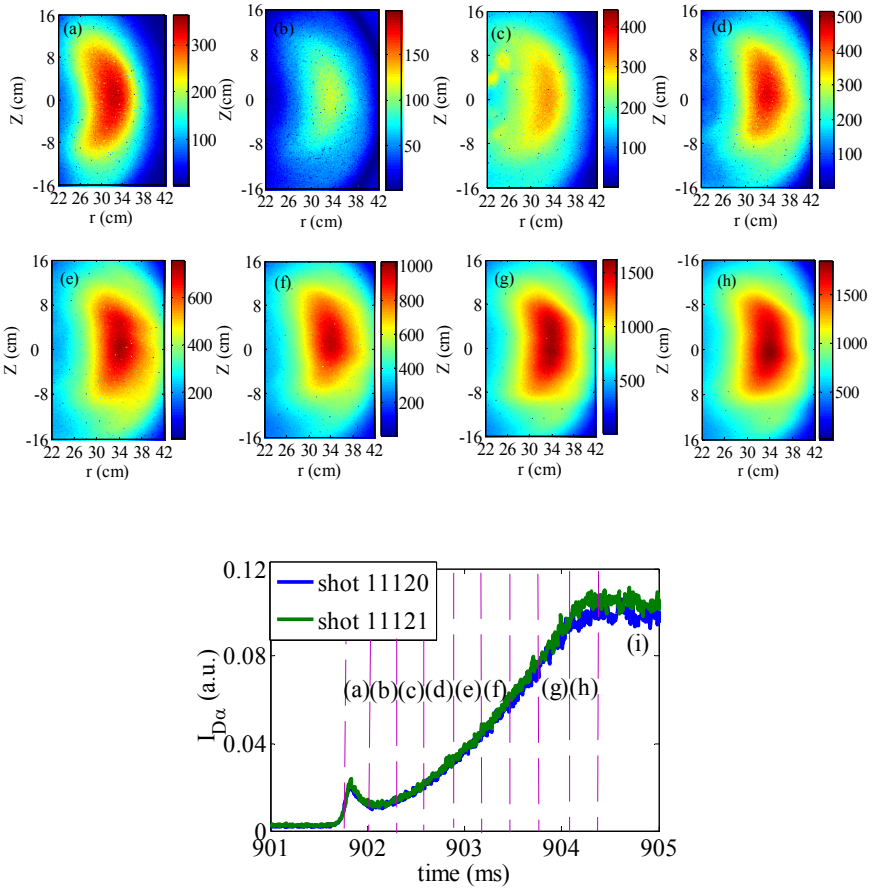

FIG. 7. The SMBI processes observed with a CCD camera and a single-channel D_α monitor. The time spans in figures (a) ~ (h) are shown in figure (i).
Due to temporal limitation of the CCD camera, each shot can be only taken one picture, therefore, figures (a) ~(h) respond to 8 shots. To ensure the reproducibility of the D_α signal, a tangential D_α detector is applied to monitor the SMBI, as shown in (i). The line averaged electron densities are $0.95\times10^{19}m^{-3}$, $1.6\times10^{19}m^{-3}$, $1.59\times10^{19}m^{-3}$, $1.93\times10^{19}m^{-3}$, $2.18\times10^{19}m^{-3}$, $1.89\times10^{19}m^{-3}$ for (a) ~ (f), and $1.74\times10^{19}m^{-3}$ for (h), respectively.

Figure 7(a) shows the spot size and deposition region of the FC, and the maximum D_α intensity of the FC is about 6 cm inside the LCFS; while the main deposition area of the SC is around 4 cm into the LCFS, as shown in figures 7(b)~(h). It is evident that the spot sizes of the FC and the initial phases of the SC (i.e. figures 7 (b) and (c)) is much smaller than that of the later phases of the SC (i.e. figures 7 (d)~(h)). The injection depth of the FC monitored by tangential D_α array is about 2 cm deeper than that by camera. Typical exposure time of the camera is 0.3 ms, which indicates the emissions to be integrated in 0.3 ms and averaged; however, the array acquires data with acquisition frequency of 200 kHz. And this may be the reason responsible for the difference between the array and camera.

Weak dependence of penetration depth on the backing pressure and the line averaged electron density before injection indicates that the penetration of the SC does not change evidently. The SC can not penetrate deeply into tokamak plasmas due to the so-called self-blocking

effect [3], which is also responsible for the different penetration depths between the FC and SC. Estimated from the velocity of the FC and SC, the directional kinetic energy of the injected molecules is less than 0.1 eV, which is much lower than that of the Frank-Condon particles; therefore, the penetration is mainly determined by the mean free path of the Frank-Condon particles disassociated from the injected molecules. For the ohmic heated HL-2A plasma, the typical edge electron density is around the magnitude of ~10^{18} m^{-3}, and the mean free path of Frank-Condon particles is of the order of decimeter. During an SC phase, however, the local plasma density increase to the order of 10^{19} m^{-3} or even higher, which makes the mean free path of the Frank-Condon particle decreases to about one centimeter. For the case of the FC, the local increment of plasma density is limited, so the self-blocking effect is not as clear as the SC phases. The self-blocking effect is elucidated well in the SMBI fuelling experiments. When the time interval between pulses is reduced to about 25 ms, the FC will be blocked by the former SC. In addition, the penetration character of the FC is similar to the beam induced by the so called bounce effect [6]. Due to the short pulse duration and hence the small amount of the injected inventory, both the FC and the beam induced by bounce inject very few particles, and hence the self-blocking effect is weaker so that they can penetrate deeper than the majority particles of the SMBI (SC).

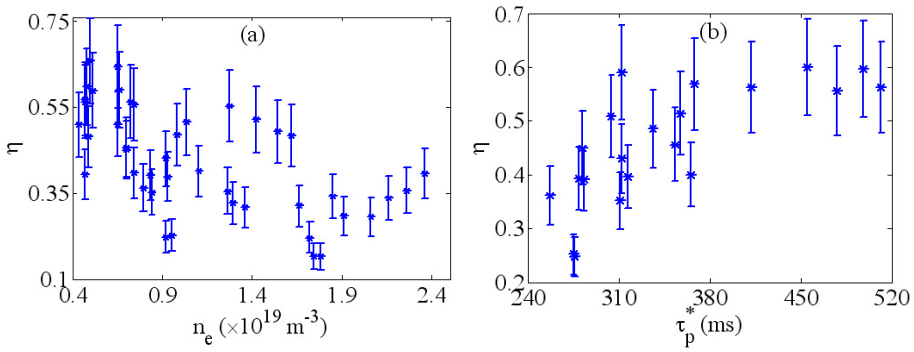

FIG. 8. The fuelling efficiency of SMBI dependent on electron density (a) and the decay time of line-averaged density (b).
Here n_e is the line-averaged electron density and τ_p^* is its characteristic decay time.

5. Fuelling efficiency

Fuelling efficiency of SMBI is also estimated, which is 30~60% for a limiter configuration on HL-2A typically, as shown in figure 8(a); and the efficiency increases with the decay time (τ_p*) of post-SMBI line-averaged density, which is closely related to the particle confinement, see figure 8(b). Since the penetration of SMBI measured with D_α array does not vary much, it is more the variation of the decay time of the post-SMBI electron density than the different injection depth that is responsible for the large scatter of the measured fuelling efficiencies.

Comparisons of SMBI fuelling efficiencies from LFS and HFS are carried out by injecting identical particles. The latter is higher than the former for the ohmic heated plasma, as shown in figure 9(a). Moreover, when the plasma is heated by the ECRH power of 1.3 MW, the fuelling efficiency drops to about half for the LFS while it decreases slightly for the HFS, as

shown in figure 9(b). The higher efficiency from HFS may be attributed to the magnetic field gradient and curvature drift effects of the ablation cloud [7]. There is always a density spike for the HFS SMBI, whereas it never appears for the LFS SMBI. During the spike, many plasma parameters, such as the edge D_α, soft X-ray and bolometer, are disturbed violently. The perturbation from HFS to plasma is higher than that from LFS.

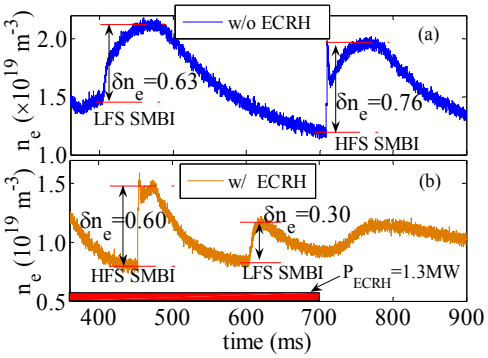

FIG. 9. Comparison of fuelling efficiency between LFS and HFS SMBIs. (a) and (b) are discharges without and with ECRH, respectively. About 3×10^{19} D_2 are injected both for LFS and HFS.

6. Discussion and summary

Based on the D_α emission, the majority particles of SMBI can penetrate about 4 cm into LCFS in HL-2A plasma with typical edge electron density of 10^{18} m^{-3}, which is shallower than the depth measured by microwave reflectometry and electron cyclotron emission. The edge cooling due to the SMBI can change the edge plasma properties, i.e. the convective drift velocity V_{in} and diffusion $D_\perp$, and hence the ratio $V_{in}/D_\perp$ becomes higher and the particle transport features changed. On the JT-60 tokamak, the same trend is observed. The maximum decrement of ion temperature T_i measured by charge exchange recombination spectroscopy locals at r/a=0.8, whereas the emission of SMBI taken by fast TV camera is mainly outside the separatrix [8]. The penetration ability of the FC is better than the SC due to weaker self-blocking effect. Among the GP, HFS and LFS SMBI, it is evident that the HFS SMBI has the highest fuelling efficiency, especially for the plasma heated by high powerful ECRH, whereas the LFS SMBI features relatively high fuelling efficiency and low perturbation to plasma.

Acknowledgments

The authors would like to express his gratitude to Professor S. Morita and Dr. X. L. Zou for their valuable discussions and suggestions. The authors would like to thank the members of the HL-2A team for operating the machine and providing the plasma diagnostics. This work was partially supported by the National Science Foundation of China under grant No. 10975049, National Magnetic Confinement Fusion Science Program under grant No. 2009GB104007 and the JSPS-CAS Core-University Program in the field of Plasma and Nuclear Fusion.

Reference

[1] Yao L. *et al* *Nucl. Fusion* **38 (**1998) 631
[2] Pégourié B. *et al J. Nucl. Mater.* **313-316** (2003) 539
[3] Lang P. T. *et al Plasma Phys. Control. Fusion* **47** (2005)1495
[4] Bucalossi J. *et al* Proc. *31st EPS Conference on Plasma Phys. London,* ECA **28G** (2004) P-4.115 (*http://epsppd.epfl.ch/London/pdf/P4_115.pdf*)

[5] Yu D. *et al Nucl. Fusion* **50** (2010) 035009
[6] Yao L. *et al Nucl. Fusion* **47** (2007)1399
[7] Parks P. B. *et al Phys. plasmas* **7** (2000) 1968
[8] Takenaga H. J. Nucl. Mater. **390-391 (**2009) 869